

# A Functional Genomics Strategy Reveals Rora as a Component of the Mammalian Circadian Clock

Trey K. Sato,<sup>1,3,7</sup> Satchidananda Panda,<sup>1,3,7</sup>  
Loren J. Miraglia,<sup>1</sup> Teresa M. Reyes,<sup>4</sup>  
Radu D. Rudic,<sup>5</sup> Peter McNamara,<sup>6</sup>  
Kinnery A. Naik,<sup>1</sup> Garret A. FitzGerald,<sup>5</sup>  
Steve A. Kay,<sup>3</sup> and John B. Hogenesch<sup>1,2,\*</sup>

<sup>1</sup>Genomics Institute of the Novartis  
Research Foundation

10675 John J. Hopkins Drive  
San Diego, California 92121

<sup>2</sup>Department of Neuropharmacology

<sup>3</sup>Department of Cell Biology  
The Scripps Research Institute  
10550 North Torrey Pines Road  
La Jolla, California 92037

<sup>4</sup>Laboratory of Neuronal Structure and Function  
Salk Institute

10010 North Torrey Pines Road  
La Jolla, California 92037

<sup>5</sup>Center for Experimental Therapeutics  
University of Pennsylvania School of Medicine  
153 Johnson Pavilion  
3620 Hamilton Walk

Philadelphia, Pennsylvania 19104

<sup>6</sup>Phenomix Corporation  
11099 North Torrey Pines Road  
La Jolla, California 92037

## Summary

The mammalian circadian clock plays an integral role in timing rhythmic physiology and behavior, such as locomotor activity, with anticipated daily environmental changes. The master oscillator resides within the suprachiasmatic nucleus (SCN), which can maintain circadian rhythms in the absence of synchronizing light input. Here, we describe a genomics-based approach to identify circadian activators of *Bmal1*, itself a key transcriptional activator that is necessary for core oscillator function. Using cell-based functional assays, as well as behavioral and molecular analyses, we identified Rora as an activator of *Bmal1* transcription within the SCN. Rora is required for normal *Bmal1* expression and consolidation of daily locomotor activity and is regulated by the core clock in the SCN. These results suggest that opposing activities of the orphan nuclear receptors Rora and Rev-erb  $\alpha$ , which represses *Bmal1* expression, are important in the maintenance of circadian clock function.

## Introduction

Circadian clocks provide an adaptive advantage by coordinating physiological, behavioral, and biochemical events to appropriate times of the day (Ouyang et al., 1998; Pittendrigh and Minis, 1972). In mammals, the

suprachiasmatic nuclei (SCN) of the hypothalamus harbor a master clock that synchronizes autonomous clocks resident in peripheral tissues, such as the liver, kidney, and heart (Hastings et al., 2003; Reppert and Weaver, 2002). Mechanistic and genetic studies have shown that the transcriptional activators Clock and *Bmal1* heterodimerize and bind E box DNA elements within the promoters of the *Period* and *Cryptochrome* genes (Etchegaray et al., 2003; Gekakis et al., 1998; Hogenesch et al., 1998). Per and Cry proteins then associate with the Clock/*Bmal1* complex to repress their own transcription, forming a 24 hr long feedback loop, a general mechanism conserved in many organisms (Dunlap, 1999; Panda et al., 2002b; Young and Kay, 2001). In addition to oscillations in Per and Cry levels, *Bmal1* also displays circadian regulation of its steady-state mRNA levels (Lee et al., 2001; Shearman et al., 2000), which is controlled in part by the orphan nuclear receptor Rev-erb  $\alpha$  (Preitner et al., 2002). Rev-erb  $\alpha$  functions as a transcriptional repressor that contributes to the trough expression of *Bmal1*. Mice with loss-of-function mutations in the *Rev-erb*  $\alpha$  gene express constitutively elevated levels of *Bmal1*, which may in turn cause shortened locomotor activity rhythms. Furthermore, cyclical Rev-erb  $\alpha$  expression is dependent upon Clock and *Bmal1*, thus forming an additional regulatory feedback loop that is thought to be important for the precision of the core oscillator.

Recently, a similar transcriptional regulatory mechanism was uncovered in the *Drosophila* circadian clock within the lateral neurons, the sites of the master oscillator in flies that are analogous to the mammalian SCN (Cyran et al., 2003; Glossop et al., 2003). In contrast to the mammalian oscillator, *Drosophila* CLOCK (dCLK) expression is cyclical, while expression of CYCLE (CYC), the *Bmal1* ortholog, remains constant. Circadian expression of dCLK is driven by cyclical and reciprocal activities of the basic leucine zipper (bZIP) transcription factors VRILLE (VRI) and PDP1. Both VRI and PDP1 can bind to a VRI/PDP1 binding site within the dClk promoter to repress or activate transcription, respectively. Mutations in *vri* and *Pdp1* affect rhythmic locomotor activity, as well as dCLK expression levels. Furthermore, circadian expression of *vri* and *Pdp1* requires dCLK/CYC, thereby connecting the dPER/dTIM and VRI/PDP1 feedback loops. However, mouse *Pdp1* homologs do not appear to be required for core oscillator function (Cyran et al., 2003), and the precise circadian *trans*-activators that drive *Bmal1* expression have not yet been identified.

Recently, we and others performed genome-wide gene expression analyses using high-density DNA microarrays to identify rhythmically expressed genes in the mouse SCN, liver, and heart (Akhtar et al., 2002; Panda et al., 2002a; Storch et al., 2002; Ueda et al., 2002), as well as kidney and aorta (R.D.R. and G.A.F., submitted; gene expression profiles are available at <http://expression.gnf.org/circadian>). Of the hundreds of cycling genes that were identified, approximately fifty genes displayed cyclical expression across multiple tissues (“cross-tissue cycling genes”; Supplemental Table

\*Correspondence: hogenesch@gnf.org

<sup>7</sup>These authors contributed equally to this work.

S1 at <http://www.neuron.org/cgi/content/full/43/4/527/DC1>). These included known oscillator components: *Cry1*, *Per2*, and interestingly, *Bmal1* and its transcriptional repressor, *Rev-erb α*. Prompted by this observation, we hypothesized that a circadian transcription factor responsible for activating *Bmal1* expression may also be included within this list of cross-tissue cycling genes. Thus, we performed functional cell-based screens to test the activities of these candidate genes on the expression of a *Bmal1* transcriptional reporter. Behavioral and molecular analyses indicate one of these activators, *Rora*, as a component of the master oscillator in mammals.

## Results and Discussion

### Identification of Orphan Nuclear Receptors as Activators of *Bmal1* Expression

We hypothesized that circadian *Bmal1* expression may be influenced by an activator(s) that cycles in several core and peripheral tissues. Of the cross-tissue cycling genes that we identified, we were able to obtain 30 corresponding full-length cDNA clones. In addition, we obtained nine cDNAs representing genes with circadian expression patterns in three out of four tissues, as well as related family members with circadian expression in at least one other tissue to compensate for low signal-to-noise ratios in the array experiments. To identify activators, HeLa cells were transfected with individual cDNAs and the *Bmal1::luciferase* (*Bmal1::luc*) reporter construct. Three cDNAs activated the *Bmal1::luc* reporter greater than 3-fold (Figure 1). Cotransfection of *Rora* or *Rorc* resulted in approximately 16- or 5-fold higher *Bmal1* expression levels, respectively, over the empty expression vector. Cotransfection of *Rorb* failed to alter *Bmal1* reporter expression, perhaps due to its inactivity in cell lines of nonneuronal origin (Greiner et al., 1996). In addition, a more than 40-fold increase in luciferase activity was seen with cotransfection of the CCAAT/Enhancer binding protein  $\alpha$  (*C/ebp $\alpha$* ), a transcription factor known to have promiscuous activities on multiple promoters (McKnight, 2001). Importantly, cotransfection of *Rora*, *Rorc*, or *C/ebp $\alpha$*  with empty pGL3-Basic or pGL3P reporter vectors did not activate luciferase expression (data not shown).

Surprisingly, no cDNA repressed *Bmal1::luc* reporter activity, which may reflect the exclusion of repressor elements (as well as activator sites) from the 530 bp promoter region used for the screen, or deficient expression of a required cofactor in HeLa cells. An alternative explanation is that low basal reporter activity, which was only 2-fold greater than that in untransfected cells (data not shown), did not allow for detection of the minimal fold change in activity. This was likely why *Rev-erb α*, which has been shown to function as a repressor on the *Bmal1* ROR element (Preitner et al., 2002), was not identified in the cell-based assay.

### *Ror* Activity Is Dependent upon Binding to the ROR Element in the *Bmal1* Promoter

*Ror* and *Rev-erb* proteins are members of the retinoic acid-related orphan receptor (ROR) family with DNA binding domains that directly interact with ROR ele-

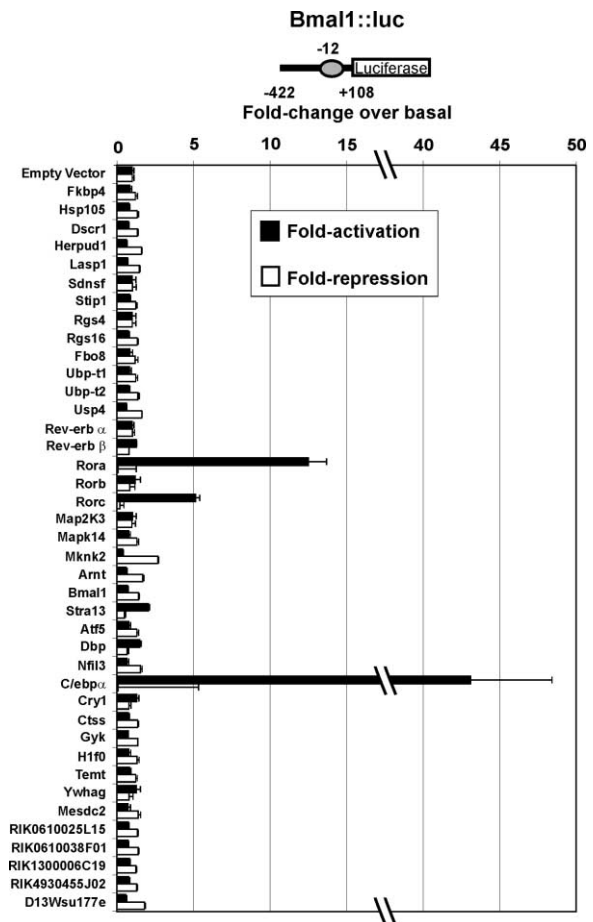


Figure 1. Functional Identification of Retinoic Acid-Related Orphan Nuclear Receptors as Activators of *Bmal1*

The bar graph indicates relative luciferase activity levels from HeLa cells cotransfected with empty vector or cDNAs from the GNF clone collection along with the pGL3Basic-*Bmal1* (*Bmal1::luc*) reporter. The gray oval represents the ROR response element within the *Bmal1* reporter construct. Numbers below the diagrams indicate starting and ending positions of the promoter sequence relative to the start of transcription, while the number above indicates the position of the ROR element. Normalized luciferase activities were plotted as fold activation (closed bars) or fold repression (open bars) relative to normalized activity in *Bmal1::luc* + empty vector transfected cells. Values shown are representative averages + standard error of the mean (SEM) of triplicate transfections from one of two experiments.

ments (RORE consensus sequence, A[A/T]NT[A/G]GG TCA, where N is any nucleotide) as monomers (Jetten et al., 2001). Interestingly, the *Bmal1* ROR element alone has been shown to confer cyclical gene expression in vitro (Ueda et al., 2002), suggesting that *Bmal1* activation may be driven by cyclical *Ror* binding and activation of the RORE and prompting us to focus on *Rora* and *Rorc* as candidates for *Bmal1* activation. We constructed wild-type and mutant RORE versions of the *Bmal1* reporter and found that *Ror* activity was significantly reduced on a mutant *Bmal1* reporter harboring a point mutation in the consensus RORE (Figure 2A). Activation by either of the two known *Rora* isoforms in mice, *Rora1* and *Rora4*, or *Rorc* was reduced 2.2-, 2.2-,

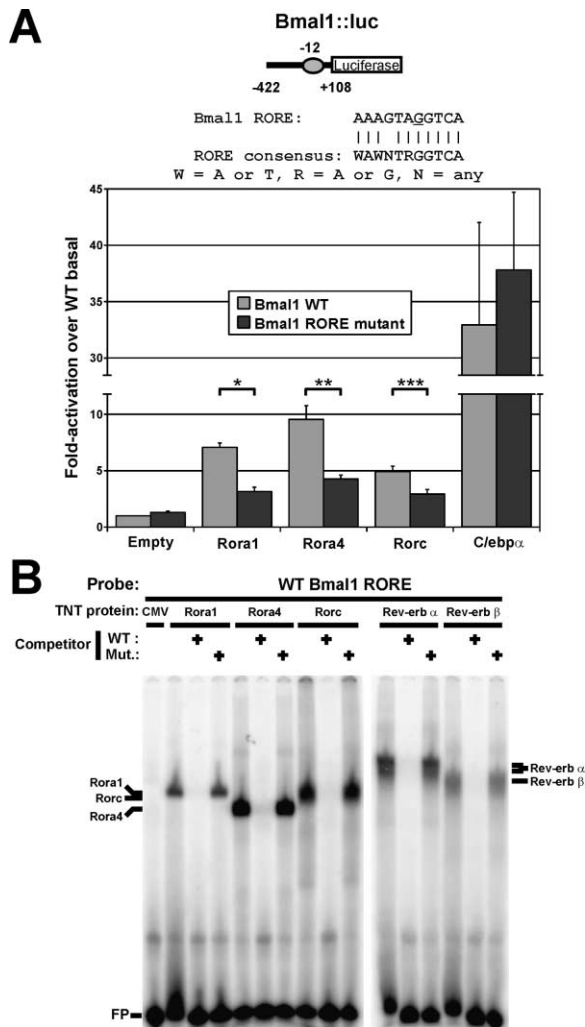


Figure 2. Rora Functions on the Bmal1 Promoter through Binding the ROR Element

(A) HeLa cells transfected with either wild-type or RORE mutant Bmal1::luc reporter and the indicated cDNA. The bar graph depicts normalized luciferase activities plotted as fold activation + SEM relative to Bmal1::luc + empty vector from three independent experiments. Comparison of the Bmal1 ROR element to the consensus RORE DNA sequence is shown above. The identity of the mutated nucleotide is underlined. Single, double, and triple asterisks denote statistically significant differences (Student's t test; \* $p < 0.002$ , \*\* $p < 0.005$ , and \*\*\* $p = 0.04$ ).

(B) DNA binding activities of orphan nuclear receptors were analyzed by electrophoretic mobility shift assays (EMSA). EMSAs with a  $^{32}$ P-labeled oligonucleotide containing the Bmal1 RORE were performed with approximately equimolar amounts of in vitro transcribed/translated (TNT) Rora1, Rora4, Rorc, Rev-erb  $\alpha$ , or Rev-erb  $\beta$ . TNT Rev-erb  $\alpha$  forms a doublet with the Bmal1 RORE probe. Binding site specificities were determined by competing the labeled probe with 1000-fold molar excess of unlabeled wild-type (wt) or mutant RORE oligonucleotides. Bands corresponding to free probe (FP) are indicated.

or 1.6-fold, respectively, with the mutant Bmal1 reporter compared to the wild-type reporter. Importantly, this mutation did not affect activation by C/ebp $\alpha$ , which likely activates through different elements, such as the many CCAAT sequences housed within the Bmal1 promoter. We further tested this possibility by performing electro-

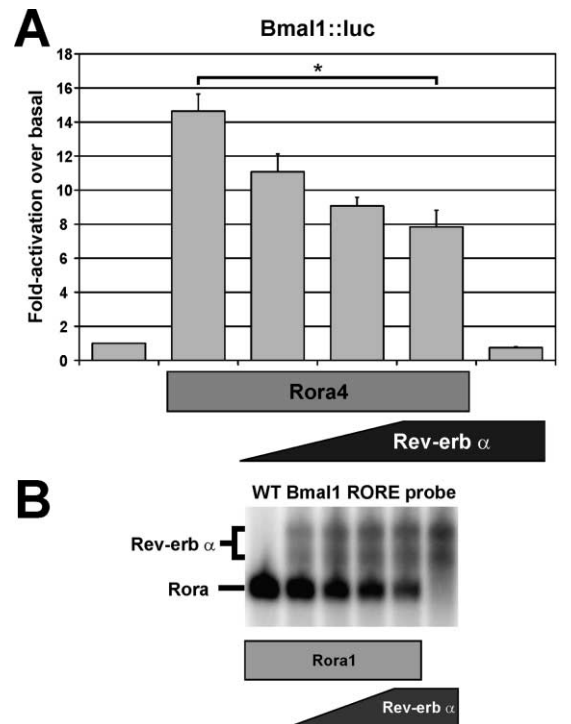


Figure 3. Rora and Rev-erb  $\alpha$  Have Functionally and Physically Antagonistic Activities on the Bmal1 Promoter

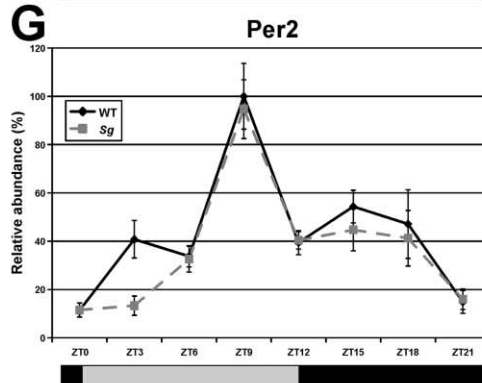
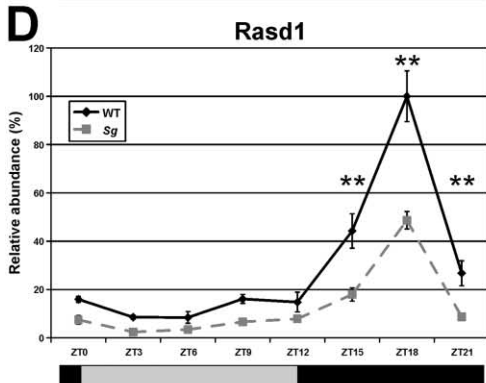
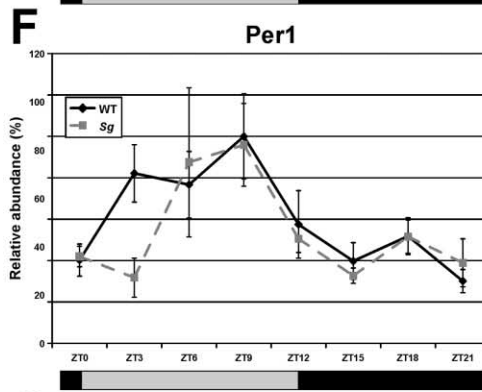
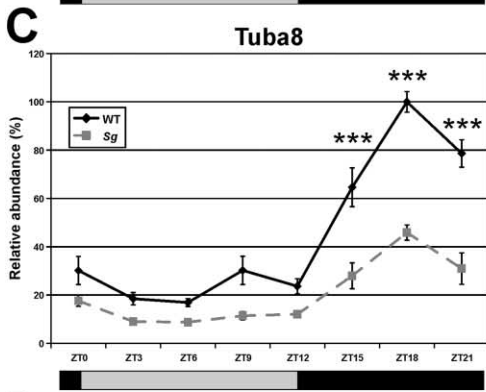
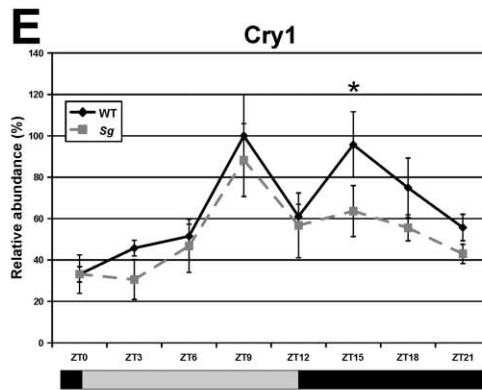
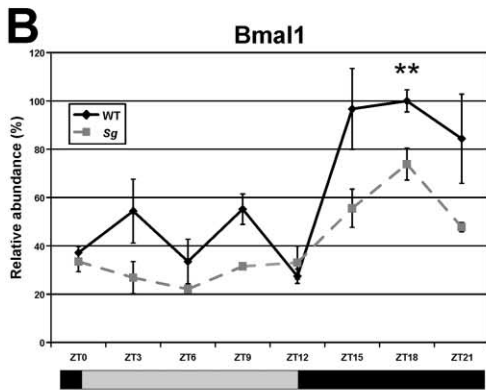
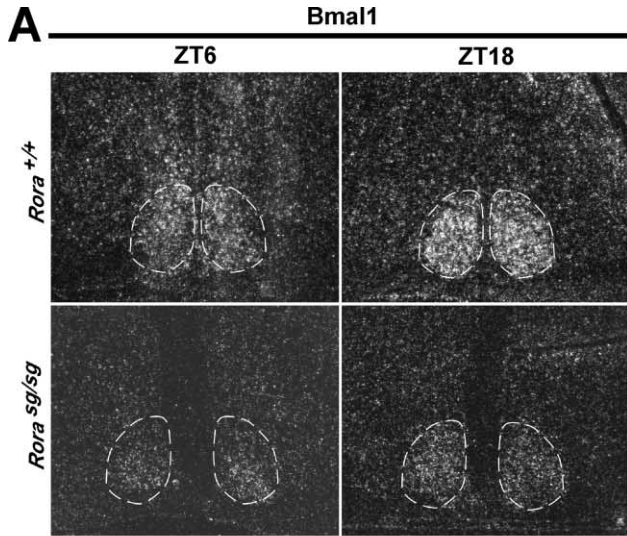
(A) HeLa cells transfected with Bmal1::luc and Rora4 were additionally cotransfected with increasing amounts of Rev-erb  $\alpha$ . The bar graph depicts normalized luciferase activities plotted as fold activation + SEM relative to Bmal1::luc + empty vector from three independent experiments. Single asterisk denotes statistically significant differences (Student's t test; \* $p = 0.03$ ).

(B) Direct competition between Rora and Rev-erb  $\alpha$  for the Bmal1 ROR element was assessed by EMSA. A fixed amount of in vitro transcribed/translated Rora1 and increasing amounts of Rev-erb  $\alpha$  (0.25-, 0.5-, 1-, and 2-fold molar excess over Rora1) were incubated with the labeled Bmal1 RORE probe.

phoretic mobility shift assays (EMSA) with a radiolabeled DNA probe containing the Bmal1 RORE incubated with in vitro transcribed and translated Rora1, Rora4, Rorc, Rev-erb  $\alpha$ , or Rev-erb  $\beta$ . All five orphan nuclear receptors formed specific complexes on the Bmal1 ROR probe, which were not seen with unprogrammed reticulocyte lysates (Figure 2B). Importantly, these complexes were specifically competed by excess unlabeled RORE oligonucleotide, while a mutant RORE oligonucleotide did not compete with the wild-type probe for binding of the specific complexes. Thus, Ror activation of Bmal1 in vitro occurs through interactions with the ROR element in the Bmal1 promoter.

#### Ror and Rev-erb $\alpha$ Functionally and Physically Compete for Binding to the Bmal1 ROR Element

As with the Ror family, both Rev-erb  $\alpha$  and Rev-erb  $\beta$  expression have been shown to cycle in the SCN, liver, heart (Akhtar et al., 2002; Panda et al., 2002a; Preitner et al., 2002; Storch et al., 2002; Ueda et al., 2002), kidney, and aorta (see above). Interestingly, the trough of circadian Bmal1 expression occurs at the peak time of Rev-



erb  $\alpha$  expression, while Bmal1 mRNA levels are highest at nearly the same times or just prior to peak Rora expression in the SCN and Rorc expression in the liver and kidney (Supplemental Figures S1A–S1C at <http://www.neuron.org/cgi/content/full/43/4/527/DC1>; Preitner et al., 2002; Ueda et al., 2002). These observations, along with our results determining that Ror functions through the Bmal1 ROR element, suggested that rhythmic Bmal1 expression may occur through circadian competition between Ror and Rev-erb activities. Therefore, we assessed the ability of Rev-erb  $\alpha$  to functionally antagonize the activities of Rora1, Rora4, and Rorc on the Bmal1 promoter in cotransfection assays. Transfection of increasing amounts of the Rora1, Rora4, and Rorc expression plasmids resulted in dose-dependent activation of the Bmal1::luc reporter (data not shown). In the presence of a fixed amount of Rora4 cDNA, additional cotransfection of increasing amounts of the Rev-erb  $\alpha$  expression plasmid resulted in the dose-dependent reduction in Bmal1::luc reporter activity (Figure 3A). Rev-erb  $\beta$  also antagonized Rora4-mediated activation (Supplemental Figure S2B at <http://www.neuron.org/cgi/content/full/43/4/527/DC1>), and both Rev-erb  $\alpha$  and  $\beta$  similarly antagonized Rora1 and Rorc activities (Supplemental Figures S2A and S2B at <http://www.neuron.org/cgi/content/full/43/4/527/DC1>). Furthermore, we directly assessed physical competition between Ror and Rev-erb  $\alpha$  for the Bmal1 ROR element by performing EMSAs with a fixed amount of Rora1 and increasing amounts (0.25-, 0.5-, 1-, and 2-fold molar excess over Rora1) of Rev-erb  $\alpha$  (Figure 3B). The addition of higher amounts of Rev-erb  $\alpha$  resulted in increased formation of the Rev-erb  $\alpha$  complex on the Bmal1 probe, along with the progressive reduction in Rora1 binding to the ROR element. Similar antagonism was seen with Rora4 and Rorc (data not shown). Thus, the cell-based functional assay and EMSA results together suggest that Rors and Rev-erb  $\alpha$  can compete for binding to the ROR element on the Bmal1 promoter to regulate its expression.

#### Mutations in Rora Affect Expression of Bmal1, Tuba8, Rasd1, and Cry1 in the SCN

Prompted by our molecular findings indicating a role for Ror family members in the regulation of Bmal1 expression, we hypothesized that loss-of-function mutations in Rora or Rorc would result in reduced Bmal1 expression in the SCN or peripheral tissues, respectively. We tested this hypothesis by analyzing Bmal1 expression in the SCN of a mouse strain, *staggerer*, which contains a mutation in the Rora gene that results in a frameshift deletion that causes a truncation of the gene product prior to the ligand binding domain (Hamilton et al., 1996). *staggerer* mutant mice display a cerebellar ataxia phe-

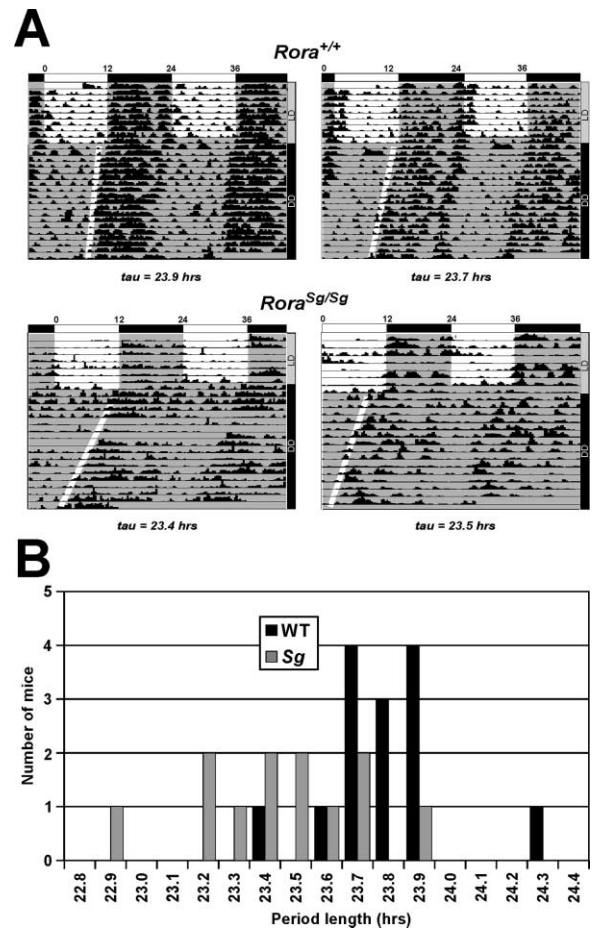


Figure 5. Mutations in Rora Result in Aberrant Locomotor Activity Rhythms

(A) Representative infrared (IR) beam-breaking double-plotted actograms of littermate *Rora*<sup>+/+</sup> (upper panels) and *Rora*<sup>Sg/Sg</sup> (lower panels) mice during entrainment (LD) and free run in constant darkness (DD) are shown. Onset of daily activity (solid white line) and period lengths ( $\tau$ ) for each individual mouse are indicated. White or gray sections of the actograms indicate periods of light or dark, respectively. Times of day in ZT (in hr) are shown along the x axis.

(B) The histogram displays the distribution of binned free-running activity period lengths as determined by IR beam-breaker assays for wild-type (black bars) and *Rora*<sup>Sg/Sg</sup> (gray bars) siblings under constant darkness.

notype resulting from defective Purkinje cell development. Comparative studies between *staggerer* and two independent transgenic Rora null mutants revealed no phenotypic differences between homozygous strains, indicating that *staggerer* is a loss-of-function mutation (Dussault et al., 1998; Steinmayr et al., 1998). Bmal1

Figure 4. Rora Is Necessary for Normal Bmal1 Expression in the SCN

(A) In situ hybridizations of coronal brain sections from wild-type and *staggerer* mice at Zeitgeber time (ZT) 6 and 18 in the first day of constant darkness (DD) were performed with a radiolabeled Bmal1 probe. Representative dark-field pictures of equivalent coronal sections are shown. Superimposed broken ovals outline the SCN. Transcript levels of Bmal1 (B), Tuba8 (C), Rasd1 (D), Cry1 (E), Per1 (F), and Per2 (G) relative to Gapdh were determined by real-time polymerase chain reaction (RT-PCR) from total RNA extracted from wild-type (wt; solid line) or *staggerer* mutant (*Sg*; broken line) SCN at the indicated ZT. Each value represents the average of three or four independent RT-PCR experiments expressed as a percentage of the maximum wild-type level for the individual gene. Asterisks denote statistically significant expression differences between wild-type and *staggerer* genotypes for the specified time point (Student's t test; \* $p < 0.05$ ; \*\* $p < 0.02$ ; \*\*\* $p < 0.001$ ).

transcript levels in the SCN of wild-type and *staggerer* mutant mice were analyzed by in situ hybridization on coronal brain sections at Zeitgeber time (ZT) 18 and 6 in the first day of constant darkness (DD), the times of peak and trough Bmal1 expression, respectively (Figure 4A). Compared to wild-type siblings, the levels of Bmal1 transcript in the SCN of *staggerer* mutants appeared to be significantly reduced at ZT18 and unchanged at ZT6.

Although the in situ studies revealed that Bmal1 levels in the SCN were reduced at the peak time of expression, it is unclear whether this reduction is the result of lower overall levels or a change in phase of Bmal1 expression. Thus, we investigated these possibilities, as well as confirmed the in situ hybridization results, by quantitative real-time polymerase chain reaction (RT-PCR) of mRNA harvested from the SCN of wild-type and *staggerer* mice at 3 hr time intervals in the first day of constant darkness. In the SCN of wild-type mice, Bmal1 expression peaked at ZT15–18 (Figure 4B), which was consistent with results from both published in situ hybridization and microarray studies (Shearman et al., 2000; Ueda et al., 2002). In contrast, Bmal1 expression between ZT15 and ZT21 was visibly reduced in the SCN of *staggerer* mutants compared to that of wild-type siblings. Together, the in situ hybridization and RT-PCR studies indicate that Rora is important for maintaining normal Bmal1 expression in the SCN.

Recently, a DNA microarray study identified a number of genes whose circadian expression patterns in the SCN closely resembled that of Bmal1 and suggested that these genes may also be directly controlled by the same transcriptional regulatory mechanism (Ueda et al., 2002). Thus, we hypothesized that loss of Rora activity may also result in abnormal expression of these genes in the SCN. In silico examination of the DNA sequences surrounding the putative transcriptional start sites (TSS) of these genes revealed that tubulin  $\alpha$  8 (Tuba8) and Rasd1/Dexas 1 both contained ROR elements within their 5' promoter regions; the Tuba8 RORE is on the reverse strand 1517 bp 5' of the TSS, while two ROR elements are housed on the reverse and forward strands 4332 bp and 2824 bp, respectively, 5' from the Rasd1 TSS. By RT-PCR, the expression of both Tuba8 (Figure 4C) and Rasd1 (Figure 4D) in the SCN of wild-type mice peaked at ZT18, similar to results described elsewhere (Ueda et al., 2002; Panda et al., 2002a). In striking contrast, both Tuba8 and Rasd1 expression were greatly reduced in the SCN of *staggerer* mice. It is interesting to note that although Bmal1, Tuba8, and Rasd1 expression are reduced, these genes still appeared to retain some rhythmic expression, suggesting the influence of other circadian factors.

While circadian expression of Per1 and Per2 is controlled primarily through Clock/Bmal1 activation of E boxes, it has been proposed that the Cry1 mRNA waveform in the liver is determined by a combination of activities from both E box and ROR elements surrounding the Cry1 TSS (Etchegaray et al., 2003). Indeed, Cry1 levels are higher in Rev-erb  $\alpha$  mutant liver at the time of peak Rev-erb  $\alpha$  expression (Preitner et al., 2002). In *staggerer* mutants, we examined Cry1 expression in the SCN and found that Cry1 was reduced at the ZT15 and ZT18 time points (Figure 4E), which corresponded to the time of peak expression of Rora target genes Bmal1,

Tuba8, and Rasd1. In contrast, at ZT9, the time of peak E box-regulated circadian expression, Cry1 mRNA levels were not different between wild-type and *staggerer* mutants. As expected, the expression of Per1 and Per2, both E box-driven targets, were unaffected in *staggerer* mutant mice in the SCN in the first day of constant darkness (Figures 4F and 4G). Expression of direct targets of Rora function, such as Bmal1, should be lower in *staggerer* mice within the first day of DD. In contrast, differences in the expression of secondary targets, such as those downstream of Bmal1, would not be seen between wild-type and mutant mice when their period length difference was shorter than the 3 hr resolution of the time course. Indeed, this may similarly explain why Rev-erb  $\alpha$  null mutants, which have a difference in locomotor period length of 0.38 hr compared to wild-type siblings (Preitner et al., 2002), do not have differences in the expression of the indirect Rev-erb  $\alpha$  targets Per2 and Cry2 within the first day in a 4 hr resolution time course. Thus, these results are consistent with the proposed model from Etchegaray et al. (2003), suggesting that both E box and ROR elements together contribute toward defining the Cry1 circadian expression pattern.

In addition to their expression in the SCN, we investigated expression of core oscillator components in *staggerer* liver. Circadian expression of Bmal1, Cry1, Per1, and Per2 in the first day of DD was not significantly affected in mutant liver (Supplemental Figures S3A–S3D at <http://www.neuron.org/cgi/content/full/43/4/527/DC1>). This was somewhat expected, because although Rora is expressed, Rora levels do not cycle in the liver (Preitner et al., 2002; Ueda et al., 2002). Rather, Rorc displayed robust circadian expression in the liver but is not expressed in the SCN of wild-type mice (Supplemental Figure S2B at <http://www.neuron.org/cgi/content/full/43/4/527/DC1>; Preitner et al., 2002; Ueda et al., 2002), and its circadian expression in the liver is maintained in *staggerer* mutants (data not shown). Thus, we suggest that oscillating levels of Rorc, whose own circadian expression could be entrained by liver-specific cues, such as feeding, can maintain circadian Bmal1 expression in the liver in the absence of a functioning SCN oscillator.

#### ***staggerer* Mutant Mice Display Defects in Circadian Locomotor Activity Consolidation**

A hallmark of all known core oscillator components in the SCN is their requirement for normal rhythmic consolidation of locomotor activity (Reppert and Weaver, 2002). Genetic defects in these components lead to alterations in period length,  $\tau$  ( $\tau$ ), or a complete loss in rhythmic activity (arrhythmicity). To determine if the described muscle coordination defects of *staggerer* mice would cause significantly reduced overall activity that could limit our detection of deficits in circadian locomotor activity, we compared a number of locomotor activity parameters between wild-type and *staggerer* mice by monitoring open field behavior and infrared (IR) beam-breaking assays. Individual wild-type and *staggerer* mutants traveled at similar average velocities during each ambulatory bout (in cm/s  $\pm$  SEM; wt,  $34.5 \pm 1.4$ ; Sg,  $39.7 \pm 2.1$ ) for similar average total distances traveled

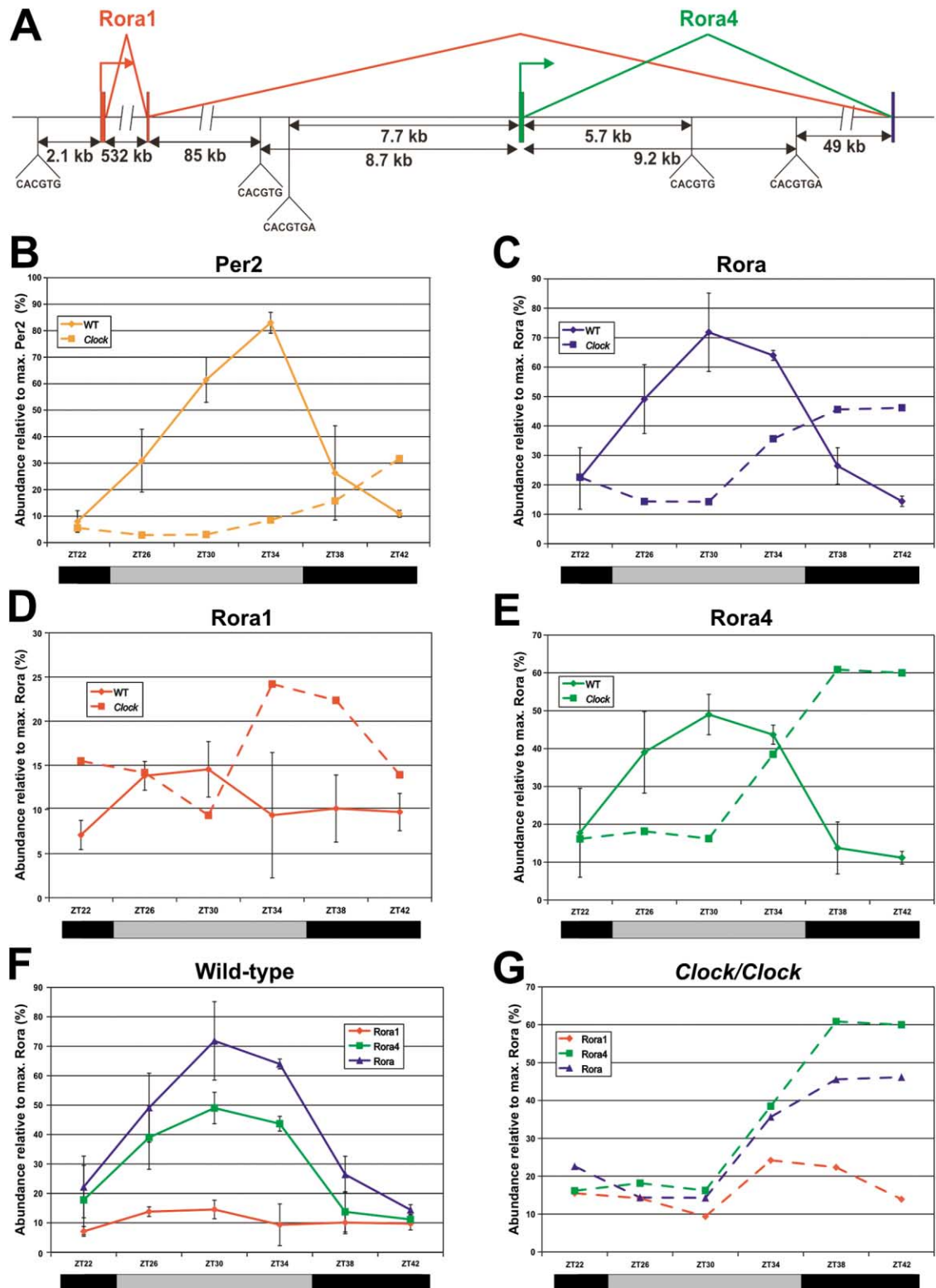


Figure 6. Clock Is Necessary for Normal Circadian Expression of Rora mRNA in the SCN

(A) Genomic organization of exons (rectangular boxes), splicing junctions (connecting triangular lines), and E boxes (CACGTG/CACGTGA) adjacent to the mouse *Rora1* or *Rora4* transcriptional start site (TSS) are depicted. Arrows projecting from exons represent the location of the TSS, and nucleotide spacing between exons is indicated in kilobases (kb). Transcript levels of *Per2* (B), *Rora* (C, F, and G), *Rora1* (D, F, and G), and *Rora4* (E-G) relative to *Gapdh* were determined by RT-PCR from total RNA extracted from wild-type (wt; solid line) or *Clock* mutant (*Clock*; broken line) SCN at the indicated ZT. Values are expressed as a percentage of the maximum wild-type expression value for *Per2* (in [B]) or *Rora* (in [C]-[G]). Each value represents the average of three or four independent RT-PCR experiments. For wild-type results, error bars denote SEM determined from two distinct biological replicates. In (F) and (G), relative transcript levels for *Rora*, *Rora1*, and *Rora4* (determined in [C]-[E]) are plotted according to genotype.

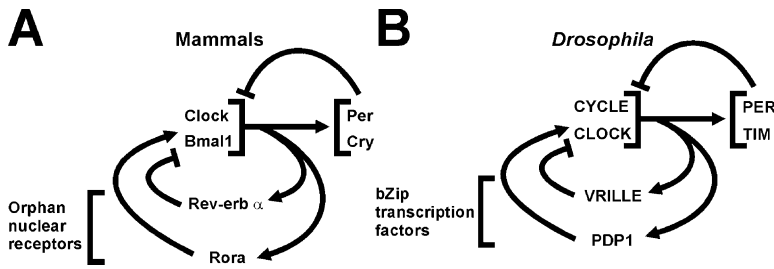


Figure 7. Mechanistically Distinct Feedback Loops in Mammals and *Drosophila* Play Key Roles in Circadian Core Oscillator Function

In flies (A), circadian expression of dCLOCK in the lateral neurons is mediated by basic leucine-zipper (bZip) transcription factors PDP1 and VRILLE, while (B) orphan nuclear receptors Rora and Rev-erb  $\alpha$  regulate circadian expression of Bmal1 in the mammalian SCN.

(in  $m \pm SEM$ ; wt,  $2.2 \pm 0.13$ ; Sg,  $2.06 \pm 0.12$ ) and with similar average total times of ambulatory activity (in  $s \pm SEM$ ; wt,  $69 \pm 4$ ; Sg,  $53 \pm 5$ ) per monitoring session. However, consistent with a defect in muscle coordination, *staggerer* mutants spent significantly less time rearing on their hind legs (in  $s \pm SEM$ ; wt,  $45.8 \pm 17.5$ ; Sg,  $2.8 \pm 3.9$ ). Furthermore, we analyzed the total daily ambulatory activities of wild-type and *staggerer* mice by IR beam-breaking assays. With this method, the total daily ambulatory (nonrepetitive, quadrant to quadrant) activities of *staggerer* mice ( $n = 15$ ; average number of ambulatory beam breaks per day  $\pm SEM = 6767.6 \pm 960.5$ ) were not statistically different from those of their wild-type siblings ( $n = 14$ ; average number of ambulatory beam breaks per day  $\pm SEM = 8878.2 \pm 1210$ ;  $p = 0.184$ ; unequal variance Student's *t* test, two-tailed distribution). Thus, while *staggerer* mice have obvious muscle coordination phenotypes, they do not have major differences in total ambulatory activity compared to wild-type mice.

We next investigated the circadian consolidation of locomotor activity in wild-type and *staggerer* mutant mice with the validated IR beam-breaking assays. These experiments revealed that *staggerer* mice had shortened locomotor activity period lengths in free-running conditions. *staggerer* mutants ( $n = 12$ ; Figures 5A and 5B) had detectable locomotor rhythms with a shortened ambulatory locomotor activity period length  $\pm SEM$  of  $23.44 \pm 0.078$  hr compared to their wild-type siblings ( $n = 14$ ; Figures 5A and 5B) with an average period length  $\pm SEM$  of  $23.79 \pm 0.054$  hr ( $p = 0.0014$ ; unequal variance Student's *t* test, two-tailed distribution). This difference in locomotor period length is not likely to be due to strain background, as these mutants had been backcrossed to C57BL/6 nine generations. In addition, free-running period lengths were not determined from free mutants (data not shown), as the precise activity onset time could not be determined. It is unclear whether these animals were arrhythmic or had unidentifiable rhythms. In sum, these behavioral experiments suggest that Rora-deficient *staggerer* mice display aberrant free-running locomotor activity rhythms.

A previous study found that null mutations in Rorb result in both ataxia and lengthened activity rhythm periods in constant darkness (Andre et al., 1998). This indicates that ataxia does not directly lead to the shortened locomotor period lengths that were observed with the *staggerer* mutants. It is intriguing that mutations in similar transcriptional activators, Rora and Rorb, would result in opposite behavioral phenotypes, analogous to the opposing period length phenotypes of Cry1 and Cry2 mutant mice (Thresher et al., 1998; van der Horst et al.,

1999; Vitaterna et al., 1999). It is equally interesting that *staggerer* mice have a similar circadian phenotype as Rev-erb  $\alpha$  repressor mutants (Preitner et al., 2002). We speculate that misregulation of Bmal1, such as the reduced amplitude of cycling, rather than its absolute levels of expression, may underlie the similar phenotypes of the *staggerer* and Rev-erb  $\alpha$  mutants. Alternatively, each of these pleiotropic transcription factors likely has distinct target genes, whose net misregulation may underlie these complex, behavioral phenotypes.

#### Normal Expression of Rora Requires Clock

Many core circadian factors are themselves direct targets of transcriptional regulation by core oscillator components, reflecting the general use of transcriptional/translational feedback regulation. The phase of Rora expression closely resembled that of two known and direct Clock/Bmal1 targets, Per1 and Per2 (Supplemental Figure S2D at <http://www.neuron.org/cgi/content/full/43/4/527/DC1>; Ueda et al., 2002). Therefore, we monitored the mRNA expression of Rora in the SCN of wild-type and *Clock* (Antoch et al., 1997; King et al., 1997) mutant mice by RT-PCR. As mentioned above, there are two known mouse Rora isoforms, Rora1 and Rora4 (see Figure 6A); Rora2 and -3 transcripts have been cloned solely from human, and the exon sequences specific to these isoforms are not present in the published mouse genome (data not shown). Utilizing primers and a probe that interrogated both mouse Rora1 and Rora4 isoforms, we found that circadian Rora expression peaked in the SCN during the daytime (ZT30; Figure 6C), consistent with published results (Panda et al., 2002a; Ueda et al., 2002). However, Rora transcript levels peaked 8 hr later in the SCN of *Clock* mutants, whose period length ( $\tau$ ) is  $\sim 27$  hr, and were visibly lower than those in wild-type mice. Per2 expression was both phase shifted by 8 hr as well as reduced in *Clock* mutant mice compared to wild-type siblings (Figure 6B). Thus, Rora has the characteristics of a first order clock-controlled gene: temporal coexpression with other direct targets of the Bmal1/Clock complex and altered expression in *Clock* mutant mice.

A difference between the Rora1 and Rora4 transcripts occurs at the 5' end, where each isoform utilizes distinct transcriptional start sites that are over 625 kb apart (Figure 6A). Specifically, the first exon of Rora4 is located within the second intron of Rora1. Upon searching for E box sequences within 10 kb 5' or 3' of the Rora1 and Rora4 TSS, one E box was found near the Rora1 TSS, while four E boxes, including two preferential Clock/Bmal1 binding E boxes, CACGTGA (Hogenesch et al., 1998), were identified near the Rora4 TSS. We then

tested whether expression of these isoforms in the SCN were dependent upon Clock function by RT-PCR with probe sets specific for Rora1 or Rora4. Rora1 and Rora4 transcripts were both detected in the SCN of wild-type mice, with Rora4 displaying the circadian expression pattern seen with the probe interrogating both Rora isoforms (Figures 6B, 6D, and 6E). Interestingly, expression of both Rora1 and Rora4 also appeared to phase shift in *Clock* mice, peaking 4–8 hr later. When relative Rora1 and Rora4 transcript levels were compared to the total Rora transcript level according to each genotype (Figures 6F and 6G), we found that Rora4 levels were 3- to 5-fold higher than Rora1 levels at peak Rora expression. Therefore, the circadianly expressed Rora4 isoform constitutes the majority of the total Rora transcript within the SCN.

Taken in sum, these results suggest that Rora is an additional component of the circadian clock in mammals and that an interplay between orphan nuclear receptors with opposing transcriptional activities maintains normal circadian expression of Bmal1 in the SCN (Figure 7A). This regulatory mechanism contrasts with that found in *Drosophila*, wherein bZIP transcription factors control the circadian expression of dCLOCK (Figure 7B; Cyran et al., 2003; Glossop et al., 2003). Thus, we suggest that the mammalian oscillator functions in an analogous but distinct manner, exploiting Ror family members in lieu of bZIP factors in the second interlocking loop. Interlocking feedback loops, then, may be a general feature of clocks that ensures robust circadian gene expression and the resulting physiological rhythms.

#### Experimental Procedures

##### Gene Profiling Analysis

mRNA extraction from mouse liver, kidney, and aorta, as well as labeling and hybridization to high-density oligonucleotide arrays, was performed as described elsewhere (R.D.R. and G.A.F., submitted; Panda et al., 2002a). Identification of genes with circadian expression patterns was performed by a cosine wave-fitting algorithm, COSOPT, as described (Panda et al., 2002a). Genes with MMC- $\beta$  values of  $<0.5$  across all four tissues were defined as putative cross-tissue cycling genes. In addition, eight genes with MMC- $\beta$  values  $<0.2$  in three out of four tissues were also included to compensate for low signal-to-noise ratios in one of the four tissues.

##### Plasmid Construction

Five hundred and thirty base pairs of the Bmal1 promoter starting at 422 base pairs upstream and ending 108 base pairs downstream of the transcriptional start were PCR amplified by Expand Long Template PCR system (Roche) from C57BL/6 mouse genomic DNA with the following primers containing flanking XhoI or SacI restriction sites: 5'-GATCGAGCTCGGGACGACGGCGAGCTCGCAGAG-3', 5'-GATCCTCGAGCGCACCCGCACTCGGATCCCG-3'. Primer designs were based upon published Bmal1 promoter sequences (Preitner et al., 2002; Yu et al., 2002). The PCR product was gel purified, digested with XhoI/SacI enzymes, and ligated into an identically cut pGL3Basic luciferase reporter vector (Promega) to generate the Bmal1::luc reporter. cDNAs from the Genomics Institute of the Novartis Research Foundation (GNF) clone collection were cloned into the pCMV-Sport6 vector (Invitrogen). All reporter constructs and cDNAs were verified by sequencing.

##### Cell Culture and Cell-Based Transcription Assays

HeLa cells (American Type Culture Collection) were maintained in Dulbecco's modified Eagle's minimal essential medium (DMEM; Gibco), 10% fetal bovine serum (FBS; Gibco), 0.1 mM nonessential amino acids (NEAA; Gibco), and Penicillin/Streptomycin/Glutamine

(PSG; Gibco) at 37°C with 5% CO<sub>2</sub>. The day before transfection, HeLa cells at 80% confluence were plated onto sterile 96-well Costar polystyrene flat bottom plates (Corning Inc.) at  $2 \times 10^4$  cells/well. The next day, the following plasmids were aliquoted as appropriate into eppendorf tubes: 25 ng Bmal1::luc reporter, 25 ng pCMV-Beta (Clontech), and 100 ng cDNA from the GNF clone collection. The pCMV-Sport6 plasmid was used as a filler to bring the total DNA concentration to 250 ng/well. The plasmids were brought to a total volume of 30  $\mu$ l with DMEM, mixed with 20  $\mu$ l of 1:20 Polyfect (Invitrogen):DMEM, and then incubated at room temperature for 10 min. After incubation, 100  $\mu$ l of DMEM/FBS/NEAA/PSG was added to the DNA, transferred onto PBS-washed HeLa cells in the 96-well plate, and then incubated at 37°C/5% CO<sub>2</sub>. Each DNA condition was conducted in triplicate for each transfection experiment. After 24 hr, transfected cells were washed with PBS and assayed for luciferase and  $\beta$ -galactosidase activities with Dual Light Kit (Tropix) according to the manufacturer's specifications. Luminescence counts were measured with an Acquest machine (LJL Biosystems). Triplicate ratios of luciferase: $\beta$ -galactosidase activities from individual transfections were averaged, and fold activations were calculated within each experimental event. Large-scale transfection screens were performed twice, while all other assays were performed at least three times. All cDNA hits from the cell-based screens were sequence verified.

##### Locomotor Activity and Open Field Behavior Assays

All animal procedures were approved by the Institute Animal Care and Use Committee of GNF in an Association for Assessment and Accreditation of Laboratory Animal Care-accredited facility. Rora<sup>sgf/+</sup> mice after nine generations of backcrosses to C57BL/6 were bred, and the progeny were genotyped. Eight- to sixteen-week-old mice were individually housed in home cages placed in the MicroMax home cage monitoring system (Accuscan Instruments, Inc.) contained within light-tight chambers at constant temperature (22°C). Rora<sup>sgf/sg</sup> mice received additional moistened food inside each cage. Mice were entrained to 12 hr of white light (800 lux white fluorescent) and 12 hr of darkness for 7–15 days and released into constant darkness (DD) for 3–4 weeks. IR beam-breaking assays were recorded using MicroMax Analyzer software (Accuscan Instruments, Inc.). Period length analyses for recorded nonrepetitive (ambulatory) IR beam breaks were performed with Clocklab and Matlab11.1 (Actimex) software. Open field behavior analyses were performed with an ENV-515 Test Environment and Open Field Activity Software (MED Associates Inc.). Wild-type (n = 11) or *staggerer* (n = 9) mice were observed for average total distance traveled, velocity, total amount of time spent moving (ambulatory activity bouts), and total amount of vertical (rearing) time in two 10 min sessions.

##### EMSA

The following complementary oligonucleotides (Gibco) were annealed to generate probes representing the ROR element (underlined; nucleotide in italics denotes mutation site) of the Bmal1 promoter: Bmal1 RORE wild-type, 5'-GAAGGCAGAAAGTAGGTCAGG GACGGAG-3' and 5'-CTCCGTCCTGACCTACTTTCTGCCTTC-3'; Bmal1 RORE mutant, 5'-GAAGGCAGAAAGTACGTCAGGGACG GAG-3' and 5'-CTCCGTCCTGACGCTACTTTCTGCCTTC-3'. Annealed wild-type RORE oligos were labeled with polynucleotide kinase (New England Biolabs) and [ $\gamma$ -<sup>32</sup>P]dATP. Labeled probes were phenol-chloroform extracted and then purified twice with MicroSpin G-25 columns (Amersham Pharmacia). One femtomole of labeled probe was incubated with in vitro transcribed/translated (TNT) reticulocyte lysate in 10 mM Hepes, pH 8.0, 1 mM EDTA, 50 mM KCl, 5 mM MgCl, 5% glycerol, 0.5 mM dithiothreitol, 2.5  $\mu$ g poly(DIdC), 1  $\times$  Complete protease inhibitor (Gibco) for 10 min at room temperature. In vitro transcription/translation of pCMV-Sport6, pCMV-Rora, pCMV-Rorc, and pCMV-Rev-erb plasmids were performed with TNT SP6 Quick Coupled Transcription/Translation System (Promega) according to the manufacturer's specifications. After incubation, protein-DNA complexes were separated by nondenaturing 5% acrylamide gel electrophoresis at 4°C and visualized by phosphorimaging. One picomole of unlabeled wild-type or mutant Bmal1 RORE oligonucleotide was incubated with radio-labeled oligonucleotide and reticulocyte lysate in competitive EMSAs. TNT protein quantifi-

cation was performed by translating in parallel with <sup>35</sup>S-methionine, separating labeled protein by SDS polyacrylamide gel electrophoresis (SDS-PAGE), and then equalizing amounts of translated protein by phosphorimaging.

#### Hybridization Histochemistry

In situ hybridization was performed using a <sup>35</sup>S-labeled antisense cRNA probe generated from nucleotides 864 to 1362 of mouse *Bmal1b* (Shearman et al., 2000). Two to three brains from adult wild-type and *staggerer* mice entrained for 7 days were removed at ZT6 and ZT18 in the first day of constant darkness and fixed in formalin for 10 days at 4°C. Fixed brains were then embedded and frozen in OCT embedding compound (Sakura Finetech). Serial coronal brain sections of 12 μm in thickness were placed and dried on glass slides. Sections were then digested with 0.1–10 μg/ml proteinase K for 30 min at 37°C. Probes were labeled to specific activities of 1–3 × 10<sup>9</sup> dpm/μg and applied to the slide at concentrations of about 10<sup>7</sup> cpm/ml, then incubated overnight at 56°C in a solution containing 50% formamide, 0.3 M NaCl, 10 mM Tris, 1 mM EDTA, 0.05% tRNA, 10 mM dithiothreitol, 1 × Denhardt's solution, and 10% dextran sulfate, after which they were treated with 20 μg/ml of ribonuclease A for 30 min at 37°C and washed in 15 mM NaCl/1.5 mM sodium citrate, at 60°C. Slides were coated with Kodak NTB-2 liquid emulsion, exposed at 4°C for 60 days, and then developed and fixed with Kodak D-19 and Kodak rapid fixer.

#### Quantitative RT-PCR

Wild-type or *staggerer* mice were entrained in 12 hr:12 hr light-dark cycles for 7–10 days. SCN and livers were dissected from four adult animals of each genotype every 3 hr during the first day of constant darkness. Total mRNA from the tissues was extracted and purified as described (Panda et al., 2002a). For SCN analysis, total mRNA was harvested from pooled tissue from four animals at each time point. Total SCN mRNA (50 ng) was converted into first strand cDNA with Superscript III (Invitrogen) and diluted 2-fold. For liver analysis, total mRNA was harvested from individual mice and pooled from two distinct biological sets of mRNA from two animals. One microgram liver mRNA was converted into first strand cDNA with Superscript II (Invitrogen) and diluted 2-fold. One microliter of cDNA was then added to 19 μl of PCR mixture (10 mM Tris-HCl, pH 8.3, 50 mM KCl, 0.2 mM dNTPs, 5 mM MgCl<sub>2</sub>, 1 unit Taq polymerase [New England Biolabs], 0.3 μM primers, and 0.4 μM probe), aliquoted into 96-well 0.2 ml thin-wall PCR plates (Biorad Laboratories), covered with optical-quality sealing tape (Biorad Laboratories), and subjected to 1 min at 95°C and then 40 cycles of 10 s at 95°C and 20 s at 60°C in an iCycler thermal cycler with the MyiQ Optical Module (Biorad Laboratories). The following forward and reverse primers and probes were designed with Primerexpress (Perkin Elmer), synthesized (Integrated DNA Technologies, Inc.), and utilized in the above reactions: *Rora* forward 5'-GCACCTGACCGAAGACGAAA-3', *Rora* reverse 5'-GAGCGATCCGCTGACATCA-3', *Rora* probe 5'-FAM-CGCGTATTTTCTGCATTCTCGT-BHQ-3'; *Rora1* forward 5'-GCGCAGGCAGCTATGC-3', *Rora1* reverse 5'-TTTCAATTTGAGATGTGTGTGCTTC-3', *Rora1* probe 5'-FAM-AGCTCCAGCCGAGGTATCTCAGTCAGC-BHQ-3'; *Rora4* forward 5'-CGCGCGCTAAAGGATGTATT-3', *Rora4* reverse 5'-CCACAGATCTTGATGGAATAATT-3', *Rora4* probe 5'-FAM-TGATCGCAGCGATGAAAGCTCAAATTG-BHQ-3'; *Per1* forward 5'-AAACCTCTGGCTGTTCTACCA-3', *Per1* reverse 5'-AATGTTGCAGCTCTCAAATACC-3', *Per1* probe 5'-FAM-ATCAACTGCCTGGACAGCATCCTC-BHQ-3'; *Per2* forward 5'-CTGCTCAGCCCTGTCTAGAA-3', *Per2* reverse 5'-AGTCAATGCTTCCAAAGTATTTGCT-3', *Per2* probe 5'-FAM-CATCCGCCACCTCAGACTCTCTGGG-BHQ-3'; *Cry1* forward 5'-CGGTTGCCTGTTTCTGACT-3', *Cry1* reverse 5'-GCTCCAATCTGCATCAAGCA-3', *Cry1* probe 5'-FAM-TCCAGCTGATCCACAGGTCACCA-BHQ-3'; *Rasd1* forward 5'-GCGCGCCTCTATCC-3', *Rasd1* reverse 5'-TCGCGGTTGTCTAAGCTGAA-3', *Rasd1* probe 5'-FAM-CACAGGAGACGTTTTCATTCTGGT-BHQ-3'; *Tuba8* forward 5'-TTGACTGGTGTCCACAGGTT-3', *Tuba8* reverse 5'-CCCTCTGGCAGCAGTAG-3', *Tuba8* probe 5'-FAM-CAAGGTGGGCATCAACTACCAGCCA-BHQ-3'; *Gapdh* forward 5'-CGTGTCTACCCCAATGT-3', *Gapdh* reverse 5'-TGTCATCATACTTGGCAGGTTTCT-3', *Gapdh* probe 5'-FAM-TCGTGGATCTGACGTGCCGCCT-BHQ-3'. Sequences for the

*Bmal1* primers and probe were published previously (Preitner et al., 2002).

Transcript levels for each gene were normalized to *Gapdh* mRNA levels and determined with the Delta-delta method (Perkin Elmer; Pfaffl, 2001). In brief, critical thresholds for each target gene were calculated by Optical System Software v1.0 (Biorad) using the maximum curvature approach. Average relative expression ratios (*R*) for each gene were calculated from three to four RT-PCR replicates and expressed as a percentage of the maximum *R* at peak expression from a wild-type sample within the time course.

#### Acknowledgments

This research was supported by the Novartis Research Foundation (to S.P., L.J.M., K.A.N., and J.B.H.); a Rena and Victor Damone Postdoctoral Fellow Fellowship from the American Cancer Society (to T.K.S.); and National Institutes of Health grants (to T.M.R. and S.A.K.). This is manuscript 15692-CB of the Scripps Research Institute. We thank Pat Chappell, Steve Reppert, and Ron Evans for plasmids; Gene Yeh, Mary Frazer, Michelle Allen, Raquel McDowell, and Susana Pires for technical support; Tony Orth for informatic analysis; Jie Zhang and John Walker for microarray support; James Watson for tissue sectioning; Mary Morrison and Colin Fletcher for *staggerer* mice; Brooke Miller, Erin McDearmon, and Joe Takahashi for *Clock* total RNA; Michael Cooke, Sumit Chanda, and Josephine Harada for critical reading of this manuscript; and Marjory Givens, Sam Hazen, Andrew Liu, and members of the Kay lab for helpful advice.

Received: January 23, 2004

Revised: June 9, 2004

Accepted: July 14, 2004

Published: August 18, 2004

#### References

- Akhtar, R.A., Reddy, A.B., Maywood, E.S., Clayton, J.D., King, V.M., Smith, A.G., Gant, T.W., Hastings, M.H., and Kyriacou, C.P. (2002). Circadian cycling of the mouse liver transcriptome, as revealed by cDNA microarray, is driven by the suprachiasmatic nucleus. *Curr. Biol.* 12, 540–550.
- Andre, E., Conquet, F., Steinmayr, M., Stratton, S.C., Porciatti, V., and Becker-Andre, M. (1998). Disruption of retinoid-related orphan receptor beta changes circadian behavior, causes retinal degeneration and leads to vacillans phenotype in mice. *EMBO J.* 17, 3867–3877.
- Antoch, M.P., Song, E.J., Chang, A.M., Vitaterna, M.H., Zhao, Y., Wilsbacher, L.D., Sangoram, A.M., King, D.P., Pinto, L.H., and Takahashi, J.S. (1997). Functional identification of the mouse circadian clock gene by transgenic BAC rescue. *Cell* 89, 655–667.
- Cyran, S.A., Buchsbaum, A.M., Reddy, K.L., Lin, M.C., Glossop, N.R., Hardin, P.E., Young, M.W., Storti, R.V., and Blau, J. (2003). *vriille*, *Pdp1*, and *dClock* form a second feedback loop in the *Drosophila* circadian clock. *Cell* 112, 329–341.
- Dunlap, J.C. (1999). Molecular bases for circadian clocks. *Cell* 96, 271–290.
- Dussault, I., Fawcett, D., Matthyssen, A., Bader, J.A., and Giguere, V. (1998). Orphan nuclear receptor ROR alpha-deficient mice display the cerebellar defects of *staggerer*. *Mech. Dev.* 70, 147–153.
- Etchegaray, J.P., Lee, C., Wade, P.A., and Reppert, S.M. (2003). Rhythmic histone acetylation underlies transcription in the mammalian circadian clock. *Nature* 421, 177–182.
- Gekakis, N., Staknis, D., Nguyen, H.B., Davis, F.C., Wilsbacher, L.D., King, D.P., Takahashi, J.S., and Weitz, C.J. (1998). Role of the CLOCK protein in the mammalian circadian mechanism. *Science* 280, 1564–1569.
- Glossop, N.R., Hou, J.H., Zheng, H., Ng, F.S., Dudek, S.M., and Hardin, P.E. (2003). *VRILLE* feeds back to control circadian transcription of *Clock* in the *Drosophila* circadian oscillator. *Neuron* 37, 249–261.
- Greiner, E.F., Kirfel, J., Greschik, H., Dorflinger, U., Becker, P., Mer-

- cep, A., and Schüle, R. (1996). Functional analysis of retinoid Z receptor beta, a brain-specific nuclear orphan receptor. *Proc. Natl. Acad. Sci. USA* 93, 10105–10110.
- Hamilton, B.A., Frankel, W.N., Kerrebrock, A.W., Hawkins, T.L., Fitz-Hugh, W., Kusumi, K., Russell, L.B., Mueller, K.L., van Berkel, V., Birren, B.W., et al. (1996). Disruption of the nuclear hormone receptor RORalpha in staggerer mice. *Nature* 379, 736–739.
- Hastings, M.H., Reddy, A.B., and Maywood, E.S. (2003). A clockwork web: circadian timing in brain and periphery, in health and disease. *Nat. Rev. Neurosci.* 4, 649–661.
- Hogenesch, J.B., Gu, Y.Z., Jain, S., and Bradfield, C.A. (1998). The basic-helix-loop-helix-PAS orphan MOP3 forms transcriptionally active complexes with circadian and hypoxia factors. *Proc. Natl. Acad. Sci. USA* 95, 5474–5479.
- Jetten, A.M., Kurebayashi, S., and Ueda, E. (2001). The ROR nuclear orphan receptor subfamily: critical regulators of multiple biological processes. *Prog. Nucleic Acid Res. Mol. Biol.* 69, 205–247.
- King, D.P., Zhao, Y., Sangoram, A.M., Wilsbacher, L.D., Tanaka, M., Antoch, M.P., Steeves, T.D., Vitaterna, M.H., Kornhauser, J.M., Lowrey, P.L., et al. (1997). Positional cloning of the mouse circadian clock gene. *Cell* 89, 641–653.
- Lee, C., Etchegaray, J.P., Cagampang, F.R., Loudon, A.S., and Reppert, S.M. (2001). Posttranslational mechanisms regulate the mammalian circadian clock. *Cell* 107, 855–867.
- McKnight, S.L. (2001). McBindall—a better name for CCAAT/enhancer binding proteins? *Cell* 107, 259–261.
- Ouyang, Y., Andersson, C.R., Kondo, T., Golden, S.S., and Johnson, C.H. (1998). Resonating circadian clocks enhance fitness in cyanobacteria. *Proc. Natl. Acad. Sci. USA* 95, 8660–8664.
- Panda, S., Antoch, M.P., Miller, B.H., Su, A.I., Schook, A.B., Straume, M., Schultz, P.G., Kay, S.A., Takahashi, J.S., and Hogenesch, J.B. (2002a). Coordinated transcription of key pathways in the mouse by the circadian clock. *Cell* 109, 307–320.
- Panda, S., Hogenesch, J.B., and Kay, S.A. (2002b). Circadian rhythms from flies to human. *Nature* 417, 329–335.
- Pfaffl, M.W. (2001). A new mathematical model for relative quantification in real-time RT-PCR. *Nucleic Acids Res.* 29, e45.
- Pittendrigh, C.S., and Minis, D.H. (1972). Circadian systems: longevity as a function of circadian resonance in *Drosophila melanogaster*. *Proc. Natl. Acad. Sci. USA* 69, 1537–1539.
- Preitner, N., Damiola, F., Lopez-Molina, L., Zakany, J., Duboule, D., Albrecht, U., and Schibler, U. (2002). The orphan nuclear receptor REV-ERB $\alpha$  controls circadian transcription within the positive limb of the mammalian circadian oscillator. *Cell* 110, 251–260.
- Reppert, S.M., and Weaver, D.R. (2002). Coordination of circadian timing in mammals. *Nature* 418, 935–941.
- Shearman, L.P., Sriram, S., Weaver, D.R., Maywood, E.S., Chaves, I., Zheng, B., Kume, K., Lee, C.C., van der Horst, G.T., Hastings, M.H., and Reppert, S.M. (2000). Interacting molecular loops in the mammalian circadian clock. *Science* 288, 1013–1019.
- Steinmayr, M., Andre, E., Conquet, F., Rondi-Reig, L., Delhaye-Bouchaud, N., Auclair, N., Daniel, H., Crepel, F., Mariani, J., Sotelo, C., and Becker-Andre, M. (1998). staggerer phenotype in retinoid-related orphan receptor alpha-deficient mice. *Proc. Natl. Acad. Sci. USA* 95, 3960–3965.
- Storch, K.F., Lipan, O., Leykin, I., Viswanathan, N., Davis, F.C., Wong, W.H., and Weitz, C.J. (2002). Extensive and divergent circadian gene expression in liver and heart. *Nature* 417, 78–83.
- Thresher, R.J., Vitaterna, M.H., Miyamoto, Y., Kazantsev, A., Hsu, D.S., Petit, C., Selby, C.P., Dawut, L., Smithies, O., Takahashi, J.S., and Sancar, A. (1998). Role of mouse cryptochrome blue-light photoreceptor in circadian photoresponses. *Science* 282, 1490–1494.
- Ueda, H.R., Chen, W., Adachi, A., Wakamatsu, H., Hayashi, S., Takasugi, T., Nagano, M., Nakahama, K., Suzuki, Y., Sugano, S., et al. (2002). A transcription factor response element for gene expression during circadian night. *Nature* 418, 534–539.
- van der Horst, G.T., Muijtjens, M., Kobayashi, K., Takano, R., Kanno, S., Takao, M., de Wit, J., Verkerk, A., Eker, A.P., van Leenen, D., et al. (1999). Mammalian Cry1 and Cry2 are essential for maintenance of circadian rhythms. *Nature* 398, 627–630.
- Vitaterna, M.H., Selby, C.P., Todo, T., Niwa, H., Thompson, C., Fruechte, E.M., Hitomi, K., Thresher, R.J., Ishikawa, T., Miyazaki, J., et al. (1999). Differential regulation of mammalian period genes and circadian rhythmicity by cryptochromes 1 and 2. *Proc. Natl. Acad. Sci. USA* 96, 12114–12119.
- Young, M.W., and Kay, S.A. (2001). Time zones: a comparative genetics of circadian clocks. *Nat. Rev. Genet.* 2, 702–715.
- Yu, W., Nomura, M., and Ikeda, M. (2002). Interactivating feedback loops within the mammalian clock: BMAL1 is negatively autoregulated and upregulated by CRY1, CRY2, and PER2. *Biochem. Biophys. Res. Commun.* 290, 933–941.